EFDA–JET–CP(12)05/18

V. Zoita, S. Soare, T. Craciunescu, M. Curuia, V. Kiptily, N. Balshaw,
P. Blanchard, D. Croft, A. Murari, B. Syme and JET EFDA contributors

Definition of the Radiation Fields for the JET Gamma-Ray Spectrometer Diagnostics

Definition of the Radiation Fields for the JET Gamma-Ray Spectrometer Diagnostics

V. Zoita[1,2], S. Soare[3], T. Craciunescu[2], M. Curuia[3], V. Kiptily[4], N. Balshaw[4], P. Blanchard[1,5], D. Croft[4], A. Murari[1,6], B. Syme[4] and JET EFDA contributors*

JET-EFDA, Culham Science Centre, OX14 3DB, Abingdon, UK

[1]*EFDA-JET CSU Culham, Culham Science Centre, Abingdon, UK*
[2]*Association EURATOM-MEdC, National Institute for Laser, Plasma and Radiation Physics, Bucharest, Romania*
[3]*Association EURATOM-MEdC, National Institute for Cryogenics and Isotope Technologies, Rm. Valcea, Romania*
[4]*EURATOM-CCFE Fusion Association, Culham Science Centre, OX14 3DB, Abingdon, OXON, UK*
[5]*Association EURATOM-CRPP-EPFL, Lausanne, Switzerland*
[6]*Association EURATOM-ENEA, RFX, Padova, Italy*
** See annex of F. Romanelli et al, "Overview of JET Results",*
(23rd IAEA Fusion Energy Conference, Daejon, Republic of Korea (2010)).

Preprint of Paper to be submitted for publication in Proceedings of the
27th Symposium on Fusion Technology (SOFT), Liege, Belgium
24th September 2012 - 28th September 2012

ABSTRACT
The JET gamma-ray diagnostics provide information on the evolution of fast particles within the tokamak configuration. Information on the spatial distribution of the interacting fast particles is obtained from the gamma-ray cameras, while energy distribution information is provided by gamma-ray spectrometers. These techniques have been successfully applied so far in fast particle simulation experiments at JET. The extension of these diagnostics to high power (high neutron yield) discharges is not straightforward. One necessary condition is to have a proper definition of the radiation (neutron and gamma) fields along the diagnostics line-of-sight. Two gamma-ray diagnostics upgrade projects at JET addressed this issue by developing neutron/gamma radiation filters ("neutron attenuators") and collimators. Neutron attenuators have been designed and constructed for the JET neutron/gamma-ray cameras and a pair of neutron/gamma collimators working in a tandem configuration have been designed and constructed for the JET tangential gamma-ray spectrometer. The tandem collimators were designed to provide collimation factors of about 5×10^2 for 2.45MeV neutrons and about 10^3 for 9MeV gamma-rays. The devices have been installed on the JET machine and the paper presents a first evaluation of the results.

1. INTRODUCTION

The control of the confinement of fast particles (in particular, the fusion reaction produced alpha particles) in the tokamak plasma is essential for the development of tokamak fusion reactors. One class of diagnostic techniques is based on the detection and analysis of the gamma radiation emitted as the result of the nuclear interactions of fast particles with plasma impurities such as C and Be [1, 2]. At JET two types of diagnostic devices address the various characteristics of the plasma emitted gamma radiation: a gamma-ray camera which provides a 2D distribution in a poloidal plane of the gamma-ray emission; a set of collimated gamma-ray spectrometers which provide gamma-ray spectra recorded along two vertical and one quasi-tangential line of sight. For the JET tokamak, gamma-ray diagnostics have been used to provide information on the characteristics of the fast ion population in plasmas [3]. The applicability of gamma-ray diagnostics to high performance deuterium and deuterium-tritium JET discharges is strongly dependent on the fulfillment of rather strict requirements for the definition and characterization of the neutron and gamma radiation fields (detector field of view, radiation shielding and attenuation, parasitic gamma-ray sources). Design solutions aimed at fulfilling such requirements have been developed for two major components of the JET gamma-ray diagnostics: the 2D gamma-ray camera [4, 5] and the gamma-ray spectrometer with a quasi-tangential line of sight [6, 7]. An upgrade of the full line-of-sight of the KM6T spectrometer was developed up to the conceptual design level [6], the main design target being the maximisation of the signal-to-background ratio at the spectrometer detector, the ratio being defined in terms of the plasma emitted gamma radiation and the gamma-ray background. This conceptual design resulted in a complex system of collimators and shields for both the neutron and gamma radiations which define the spectrometer field of view. This paper presents the first two components of the upgraded diagnostics line-of-sight, the tandem collimator system (KM6T-TC) for the KM6T tangential gamma-ray spectrometer designed with the aim of providing a well-defined field of view at the plasma end of the diagnostics line-of-sight. The collimation system should at the same time improve the signal-to-background ratio at the detector end of the line-of-sight.

2. PLASMA FIELD-OF-VIEW DEFINED BY THE KM6T TANDEM COLLIMATORS

A tandem of neutron/gamma collimators have been designed and constructed for the JET KM6T diagnostics (Fig.1). A front collimator defines the spectrometer field of view at the plasma end of the line-of-sight.

Its dimensions (outer diameter and length) have been determined in terms of the available space in front of the Octant 8 vacuum port. A rear collimator defines (by its external diameter) the radial extension of the shielded field seen by the BGO gamma-ray detector.

3. ESTIMATION OF THE EXPECTED SIGNAL-TO-BACKGROUND RATIO

In order to estimate the volume of the plasma seen by the BGO detector within the FoV defined by the tandem collimators, the following procedure was used: i) a high power, high beta plasma discharge was chosen (JET Pulse No: 62213, 21MW NBI, 4MW RF, 6.5×10^{16} neutrons) for the evaluation; ii) three of the EFIT flux surfaces were approximated by ellipses and a toroidal flux surface configuration was generated in CAD (CATIA) (Fig.4); iii) the toroidal surfaces were intersected with the KM6T conical shape FoV and iiii) the volumes of the resulting intersections were calculated in CATIA (Fig.5). A volume of approximately $0.3m^3$ resulted for the plasma seen by the KM6T gamma-ray spectrometer.

Two sources of parasitic gamma-radiation have to be taken into account for the determination of the gamma-ray background: i) neutron capture gamma-ray emission form solid targets which fall into the KM6T The thickness of the rear collimator is determined by the necessary amount of material needed to shield the BGO detector from the neutron (2.45MeV) and gamma radiation (9 MeV). Both collimators are made up of polyethylene plates for the neutron shielding and lead plates for the gamma-ray shielding. A modular structure of the two collimators allows for a straightforward extension to a configuration suitable to deuterium-tritium operation (14.1MeV neutrons).

The KM6T diagnostics field-of-view (FoV) defined by the tandem collimators within the JET vacuum vessel is shown in Fig.2. It extends from the Octant 8 vacuum port (entrance) to the Octant 3 vacuum port (exit).

In a plane that contains the Inner Wall Guard Limiter (IWGL) of Octant 2, the front collimator provides a FoV with a diameter of 407 mm, while the rear collimator FoV has a 737mm diameter (Fig.3).

FoV; ii) fast-particle induced gamma-ray emission from those surfaces ($0.17m^2$ fall in the FoV, CATIA model) of the outer poloidal limiters seen by the KM6T spectrometer. Three neutron capture sources have been identified: i) the NBI duct scraper (Cu) in Octant 8; ii) two IWGL's and their supports (Be and INCONEL) and iii): outer poloidal limiters and LH launcher (Be and INCONEL) in Octant 3.

The signal-to-background ratio expected from the FoV defined by the KM6T tandem collimators was estimated in the following way: i) the flux of fast particles falling on the outer poloidal limiters was estimated to be similar to that measured by the JET Faraday cup diagnostics; ii) the plasma gamma-ray emission rate was estimated as that observed in a fast ^{3}He RF acceleration experiment and iii) the plasma volume and the limiter surface were estimated from the CATIA model of the KM6T FoV. The signal-to-background ratio resulted to be about 10^4, a very encouraging value that should provide enough room for more precise evaluations.

4. EVALUATION OF RADIATION (NEUTRON AND PHOTON) PERFORMANCE OF THE KM6T TANDEM COLLIMATORS

The evaluation of the designed shielding characteristics of the KM6T tandem collimator assembly was performed by means of Monte Carlo numerical simulations using the MCNP-5 code. A simplified geometry that uses point (neutron and photon) sources irradiating the collimators within a defined solid angle and detectors placed behind the collimators was used for the numerical simulation [7]. Various collimator configurations were investigated and for all the cases the following parameters have been calculated within the region defined by a set of "virtual detectors": i) the integrated neutron flux; ii) the integrated flux of the photons generated by neutron capture within the collimation structure and iii) the integrated flux of the photons emitted by parasitic gamma-ray sources.

The physical performance of the collimation structure has been characterised by a shielding parameter defined as the ratio of the particle fluxes at the directly exposed and shielded virtual detectors, respectively. The point neutron source has a Gaussian shape neutron spectrum with the mean energy at $E_0 = 2.45$ for deuterium discharges and $E_0 = 14.0$MeV for deuterium-tritium discharges. A full width at half maximum (FWHM) of 0.5MeV was taken in both cases. The point photon source is represented by a single line of energy 9MeV, corresponding to the most intense nickel neutron capture gamma-ray line expected to be emitted by the INCONEL support of the Inner Wall Guard Limiter (IWGL) [6]. The results of the MCNP calculations for the 2.45MeV neutron collimator configurations were presented in [7]. This paper presents the calculations for the 14MeV configuration.

The 14MeV collimator configuration and its MCNP simplified geometry is similar to that used in [7]. Two virtual detectors are placed behind the rear collimator, one detector being placed on the tandem collimator axis, and the other in the shadow of the collimator at the mid-radius. Both detectors lie in a plane at a distance of 50mm behind the rear face of the collimator. The calculations were done for a front collimator made up of 18 alternating polyethylene (thickness 40mm) and lead (thickness 10mm) plates. The rear collimator is made up of two modules of 12 alternating polyethylene (thickness 40mm) and lead (thickness 10mm) plates. Each module has an additional 10mm lead plate at the rear face.

The radiation sources have specific positions: i) a point neutron source placed at the intersection of the tandem collimator axis with the vertical projection of the magnetic axis. This is at a distance of 4.194m from the front face of the front collimator and ii) a 9 MeV point gamma-ray source placed at the intersection of the tandem collimator axis with a plane perpendicular to the surface of the inner wall guard limiter in Octant 2. This is at a distance of 6.489m from the front face of the front collimator.

The propagation space for the simulated radiation transport was limited to a reduced solid angle in order to reduce the computation time. This was defined in terms of the angle subtended by the front face of the front collimator which was increased by a factor of 5 in order to avoid biasing of the evaluated tally.

The KM6T tandem collimator configuration designed for deuterium-tritium (DT) operation (14.1MeV neutrons) provides a shielding factor the full system of about 450 for the neutrons and about 15 for the neutron-induced photons. The shielding factor for the 9MeV parasitic gamma-ray line is about 10^3. This is to be compared with the configuration designed for deuterium discharges (2.45MeV neutrons) which provides shielding factors of about 500 for 2.45MeV neutrons, 30 for neutron-capture photons induced within the collimation structure and about 900 for a parasitic gamma-ray line of 9MeV [7].

5. INSTALLATION AND COMMISSIONING OF THE KM6T TANDEM COLLIMATORS

The two KM6T tandem collimators were manufactured during 2010 and 2011 and installed on the JET machine on the tangential gamma-ray spectrometer beam line (Fig.7). The design field-of-view defined by the tandem collimators at the plasma end of the KM6T diagnostics was confirmed by checking the alignment of the collimators during a series of surveys carried out after the installation.

The overall result shows that the tandem collimator axis is coincident with the axis of the KM6T diagnostics line-of-sight within the accuracy of the measuring instruments (millimetre and 0.1 degree displacements). This confirms the achievement of the designed field of view at the plasma (source) end of the KM6T diagnostics line-of-sight. In order to evaluate the improvement of the gamma-ray signal-to-background ration one should compare the experimental gamma-ray spectra obtained by the KM6T spectrometer in two configurations: one without the tandem collimators (e.g., JET pulses produced during the 2009 campaigns, with the carbon wall) and the other one with the tandem collimators in place (JET pulses obtained in 2012, with the beryllium wall). The installation of ITER-Like Wall (ILW) lead to gamma-ray spectra substantially different from those obtained with the carbon wall and any direct comparison turned out to be practically impossible. It was therefore necessary to find a gamma-ray spectral feature which was not strongly influenced by the new wall structure and which could be used to show the positive effect of the tandem collimators at the KM6T detector. The 2.2MeV gamma-ray line determined by the neutron capture reaction $H(n,\gamma)D$ in the polyethylene attenuator (internal attenuator), located inside the bunker wall (Fig.1), was chosen as a spectral line monitor as this should be dependent only on the neutron flux interacting with attenuator.

Two sets of pulses were selected in order to experimentally assess the performance of KM6T-TC by comparison of the recorded gamma-ray line for hydrogen neutron capture reaction. The integrated (total) neutron yield is greater than 6.5x1017 for the pulses before KM6T-TC installation and above 2.0×10^{17} for the experiments performed after KM6T-TC installation. For the 2012 JET pulses the neutron yields are only approximate values as there is no neutron calibration with the new wall. The cumulated gamma-ray spectra for the two sets of pulses are presented in Fig.8 as an illustration of the comparison procedure. The expected 2.2MeV hydrogen capture gamma-ray line is actually a superposition of two gamma-ray lines: the hydrogen capture line and a line resulting from the reaction of tritons produced by the DD fusion reactions with the beryllium impurity in the plasma.

CONCLUSIONS

Two neutron/gamma collimators working in tandem have been designed and constructed for the JET tangential gamma-ray spectrometer.

The shielding characteristics of the tandem collimators were defined in terms of a shielding factor and this was calculated for a configuration designed to be used in DT experiments. This 14MeV neutron configuration would provide shielding factors of about 450 for the neutrons and about 15 for the neutron-capture photons. The shielding factor for a 9MeV parasitic gamma-ray line would be about 10^3.

After the installation on JET of the KM6T tandem collimators their alignment with respect to the diagnostics axis was checked by a series of surveys which confirmed the achievement of the designed field of view at the plasma (source) end of the KM6T diagnostics line-of-sight.

A procedure for the assessment of the reduction in the gamma-ray background has been developed and it is to be applied after having a new neutron calibration on the JET machine.

ACKNOWLEDGMENTS

This work was supported by EURATOM and carried out within the framework of the European Fusion Development Agreement. The views and opinions expressed herein do not necessarily reflect those of the European Commission.

REFERENCES

[1]. O.N. Jarvis et. Al., Nuclear Fusion, **36**, 1513 (1996).
[2]. V.G. Kiptily et al., Nuclear Fusion, **42**, 999 (2002).
[3]. V.G. Kiptily et al., Plasma Physics and Controlled Fusion, **48**, R59 (2006).
[4]. V. Zoita, et al., Fusion Engineering and Design, **84**, 2052 (2009).
[5]. M. Curuia et al., Fusion Engineering and Design, **86**, 1196 (2011).
[6]. V. Zoita et al., 23rd SOFE, 2009, San Diego, California, USA
[7]. S. Soare et al., Fusion Engineering and Design, **86**, 1359 (2011).
[8]. I.N. Chugunov et al., Instruments and Experimental Techniques, 2008, Vol. 51, No. 2, pp. 166–170

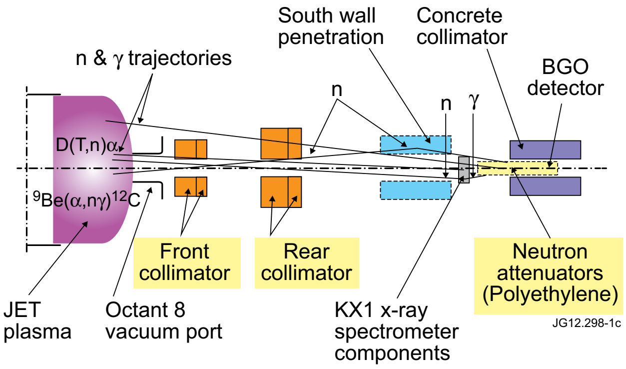

Figure 1: Schematic representation of the KM6T diagnostics configuration with the tandem collimators.

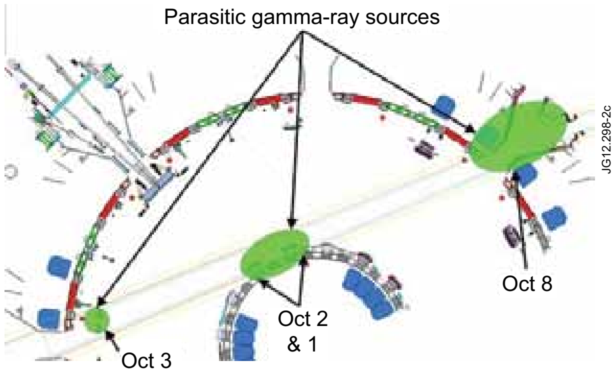

Figure 2: KM6T field-of-view defined by the tandem collimators within the vacuum vessel. Cross-section by a horizontal plane containing the KM6T axis.

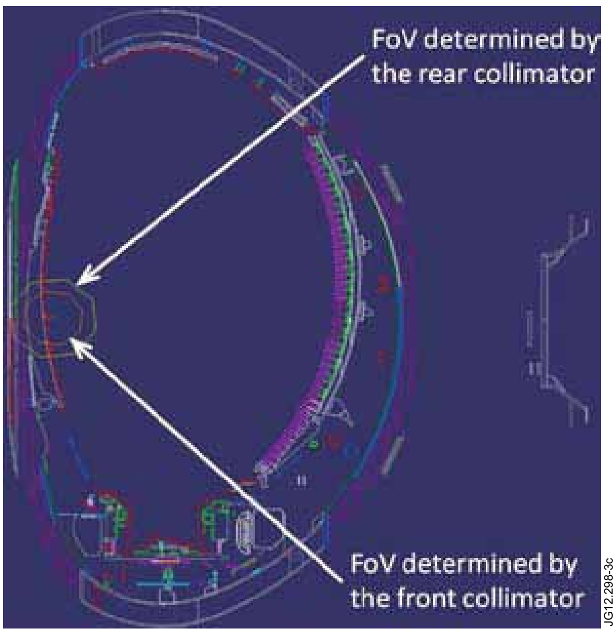

Figure 3: The KM6T FoV at the Octant 2 IWGL with respect to the vacuum vessel X-section.

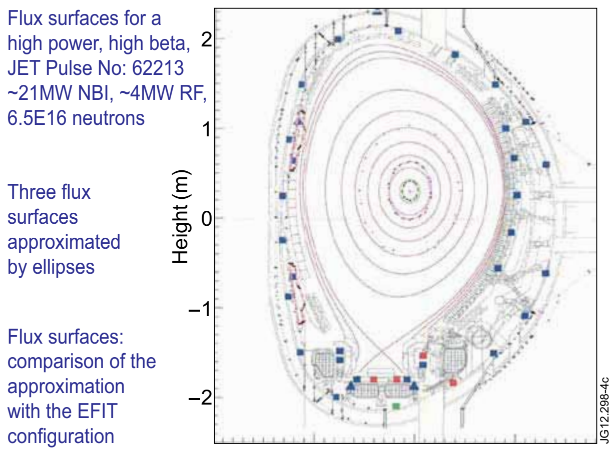

Figure 4: EFIT flux surfaces were approximated by ellipses (dotted).

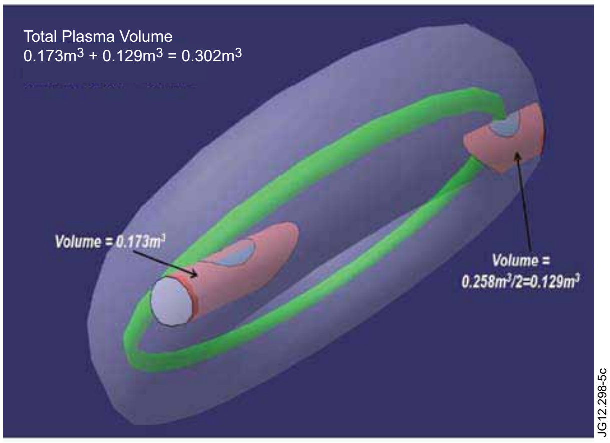

Figure 5: Plasma volumes resulting from the intersection of the toroidal flux surfaces with the KM6T FoV.

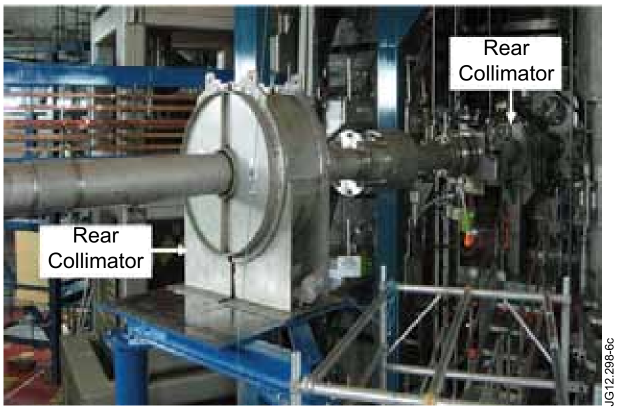

Figure 7: KM6T Tandem Collimators installed on JET.

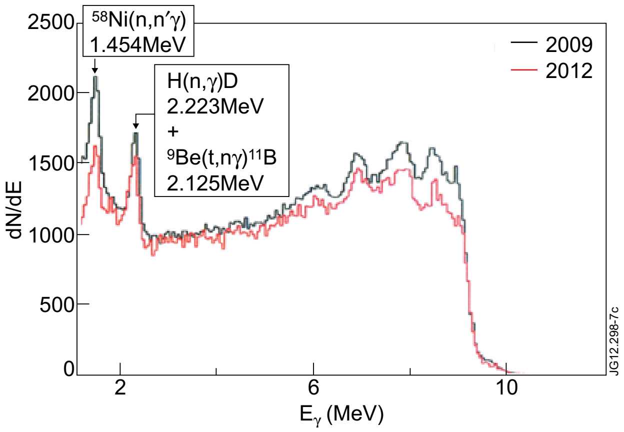

Figure 8: Comparison of cumulated spectra recorded before and after the installation of KM6T-TC.